Spectral Power Time-courses of Human Sleep EEG Reveal a Striking Discontinuity at ~18 Hz Marking the Division between NREM-specific and Wake/REM-specific Fast Frequency Activity

Helli Merica[1] and Ronald D. Fortune[2]

[1]Laboratoire de Sommeil et de Neurophysiologie, Hôpitaux Universitaires de Genève, Belle Idée, 1225 Chêne-Bourg, Geneva, Switzerland and [2]CERN European Organisation for Nuclear Research, 1211 Geneva 23, Switzerland

Spectral power time-courses over the ultradian cycle of the sleep electroencephalogram (EEG) provide a useful window for exploring the temporal correlation between cortical EEG and sub-cortical neuronal activities. Precision in the measurement of these time-courses is thus important, but it is hampered by lacunae in the definition of the frequency band limits that are in the main based on wake EEG conventions. A frequently seen discordance between the shape of the beta power time-course across the ultradian cycle and that reported for the sequential mean firing rate of brainstem–thalamic activating neurons invites a closer examination of these band limits, especially since the sleep EEG literature indicates in several studies an intriguing non-uniformity of time-course comportment across the traditional beta band frequencies. We ascribe this tentatively to the sharp reversal of slope we have seen at ~18 Hz in our data and that of others. Here, therefore, using data for the first four ultradian cycles from 18 healthy subjects, we apply several criteria based on changes in time-course comportment in order to examine this non-uniformity as we move in 1 Hz bins through the frequency range 14–30 Hz. The results confirm and describe in detail the striking discontinuity of shape at around 18 Hz, with only the upper range (18–30 Hz) displaying a time-course similar to that of the firing-rate changes measured in brainstem activating neurons and acknowledged to engender states of brain activation. Fast frequencies in the lower range (15–18 Hz), on the other hand, are shown to be specific to non-rapid-eye-movement sleep. Splitting the beta band at ~18 Hz therefore permits a significant improvement in EEG measurement and a more precise correlation with cellular activity.

Keywords: beta band limits, brainstem–thalamic activating neurons, neuronal transition probability model, spectral analysis, spindles

Introduction

A number of studies at cellular level have focused on the modulatory control of sleep states by brainstem–thalamic activating neurons and have provided time-course data on their firing rate comportment (Steriade, 1984; Steriade *et al.*, 1990). Some insight into this modulatory control is also provided by the neuronal transition probability (NTP) model deduced from the relationships between the time-courses of power in the different frequency bands of the sleep electroencephalogram (EEG) (Merica and Fortune, 2000, 2003). The subcortical and EEG data together thus offer the possibility of relating their concurrent dynamics and of providing a fuller and more unified picture of the sleep process (Merica and Fortune, 2004). A coherent integration of data from the two levels of investigation depends on precision of sleep EEG measurement and this in turn depends on the assignment of precise band limits — in particular, for the fast frequencies. These limits have a strong influence on the resulting time-courses, especially the choice of the lower limit. This is because EEG spectra, after the slow oscillation maximum at ~0.8 Hz, follow an ~$1/f$ decay law, i.e. the lower the frequency, the higher the power. This will inevitably weight the time-course shapes of any particular band in the direction of the shapes associated with the lower frequencies. Unfortunately, there is little consensus either on the precise definition of these limits or on empirical criteria that could help to derive them. For example, beta band limits in sleep are traditionally based on conventional wake EEG definitions that take no account of the fact that the shapes of the spectral power time-courses in the beta range (15–30 Hz) show a sharp discontinuity with frequency at ~18 Hz (Fig. 1). Therefore, treating the beta range as a single band will mix the negative starting slopes above 18 Hz with the higher-powered positive starting slopes below and lead to imprecise results for the shape of the time-courses. Yet, although some studies circumvent the problem of band limit definition by adopting a 1 Hz resolution approach (e.g. Aeschbach and Borbély, 1993; Finelli *et al.*, 2001; De Gennaro *et al.*, 2002), the majority of spectral analysis studies in sleep orient their conclusions on traditionally defined limits. To the best of our knowledge there has been only one systematic study that has attempted to resolve the band limit issue in sleep (Lanquart, 1998), but the sampling rate used was unfortunately too low to enable firm conclusions to be drawn on the fast frequency beta range.

The beta frequencies are of particular interest because of their long association in neurophysiology with states of cortical arousal such as wake and rapid-eye-movement (REM) sleep — and a reluctance in the field to conceive that they may also occur during a non-rapid-eye-movement (NREM) episode, a deafferented sleep state. Nevertheless it has been shown that these higher frequencies appear superimposed on the cortically generated slow oscillation in both anaesthetized and normally sleeping cats (Steriade *et al.*, 1996; Steriade, 2001). EEG researchers have long been aware of the presence of beta throughout the NREM episode (e.g. Uchida *et al.*, 1992; Aeschbach and Borbély, 1993; Merica and Fortune, 1997) but in general have focused less attention on these frequencies. Cellular neurophysiology findings indicate that as we go towards deep NREM sleep, the firing rates of brainstem–thalamic activating neurons and cortically projecting basal forebrain neurons progressively decrease, mirroring the gradual firing-rate increase of the sleep-promoting neurons located in the ventrolateral preoptic region (Szymusiak *et al.*, 1998; Saper *et al.*, 2001). As a result, thalamocortical (TC) neurons become gradually more hyperpolarized, leading first to light and then to deep sleep. Conversely, increased brainstem excitatory input depolarizes the TC cells, leading either to waking or REM sleep (Steriade and

McCarley, 1990; Steriade *et al.*, 1993a). The time-course of this excitatory input over the NREM episode is generally U-shaped (Steriade *et al.*, 1990), and this is reflected at the EEG by the similar comportment of fast frequency (beta) activity (see fig. 1 in Merica and Fortune, 2003). Research until now has generally adopted a single beta band with a lower limit 15–16 Hz and an upper limit 25–35 Hz (Uchida *et al.*, 1992; Aeschbach and Borbély, 1993; Mann *et al.*, 1993; Merica and Blois, 1997; Finelli *et al.*, 2001; De Gennaro *et al.*, 2002). This has led to some imprecision in time-course results for beta, particularly at the start and at the end of NREM: we noted in previous studies using traditional beta limits the larger spread in beta power (and incidentally the lower quality of fit to the NTP model) particularly at the NREM extremities (Merica and Fortune, 1997, 2000). Some recent results have serious discrepancies in regard to the U-shape expected from cellular work, with beta power rising instead of falling at the start of NREM and falling instead of rising at the end (see fig. 2 in De Gennaro *et al.*, 2002). The reason for such discrepancies is suggested by the spectral power time-course comportment seen in several studies. In one penetrating study, Uchida *et al.* (1992) showed that activity in the traditional beta range 15–28 Hz is 'non-uniform in its relationship with delta activity', with only the 20–28 Hz part of the range displaying 'a consistent inverse relationship across both NREM and REM'. Since the delta power time-course is arch-shaped across the NREM–REM cycle, the non-uniformity strongly suggests that there is a significant change in the beta time-course comportment at ~20 Hz, with only the upper range exhibiting a U-shaped time-course similar to that of the brainstem–thalamic activating neurons. Although the authors state that their 15–23 Hz range 'has an inconsistent time-course behaviour, sometimes behaving like sigma and sometimes as the 20–28 Hz band', they have little to say about the origin of this inconsistency. Also, Aeschbach and Borbély (1993) clearly showed in their data a sharp discontinuity with frequency in the character of the average beta time-course, at ~18 Hz (Fig. 1). Focusing on the left side of their diagram and proceeding from high to low frequency, we see that the beta power suddenly switches in both amplitude and slope from a high start and negative slope above 18 Hz to a low start and positive slope below. Although the authors make no mention of this discontinuity, we believe that it is of fundamental importance and lies behind the anomalies mentioned above.

The aim of the present study is therefore to make a systematic investigation in a broad frequency range centred on 18 Hz in order to pinpoint the exact location and inter-subject distribution of the discontinuity, and to give some indication of its implications for time-course measurement. Equally important is to place this discontinuity in the context of cellular observations and the NTP model.

Materials and Methods

Subjects
The study uses data from 18 healthy paid volunteers aged between 20 and 30 years (24.6 ± 2.8 years) from whom informed consent was obtained in accordance with local Ethical Committee requirements. The data were selected randomly from our data bank of all-night drug-free sleep recordings carried out under controlled environmental conditions. Bedtimes were scheduled from 21:30 to 07:00 h. All subjects were screened for good health on the basis of their history and clinical examination and the absence of any sleep disturbances determined on the basis of a first night polysomnography that also served as a habituation night. Subjects were asked to refrain from drinking more than two cups of coffee or more than two glasses of wine per day in the week preceding nocturnal recording and to abstain from the consumption of both beverages over the recording period.

EEG recording, Data Extraction and Spectral Analysis
All-night sleep was recorded using three bipolar EEG derivations (F4–Cz, C4–T4 and Pz–O2), one horizontal electrooculogram, one submental electromyogram, an electrocardiogram and respiration (monitored by thermistors under the nostrils). Sleep stages were visually scored every 20 s using Rechtschaffen and Kales rules (Rechtschaffen and Kales, 1968). Signals from the F4–Cz derivation used in this study were high-pass and low-pass filtered (0.5 and 70 Hz) and digitized at a sampling rate of 256 Hz with 12-bit resolution. Prior to analyses, the signals were subjected to an automatic one-second-resolution artefact detection routine using a background-dependent filter based on the root mean square amplitude of the signals. After visual validation, all epochs containing artefacts were coded as missing data so as to preserve time continuity. Power spectra in units of μV^2 were computed by fast Fourier transform with a Hanning window for consecutive 4 s epochs, giving a 0.25 Hz resolution over a frequency range 14–30 Hz, adequate to cover the traditional beta range. Four consecutive elementary bins of width 0.25 Hz were integrated to give the 1 Hz resolution interval used in this study. All frequency ranges are defined here in the same way: '15–18 Hz', for example, signifies that the first constituting interval starts at 15 Hz and the last ends at 18 Hz. Sleep staging and signal analysis, as well as the preliminary artefact rejection, were done using the PRANA package from PHITOOLS Grenoble, France.

REM and NREM episodes were separated using the 15 min combining rule for defining the end of a REM episode (Feinberg and Floyd, 1979; Merica and Gaillard, 1991). No minimum duration of REM sleep was required in order to define the start of a REM episode. The start of the first NREM episode was set at sleep onset defined as the first appearance of stage 2 sleep. The epoch that immediately follows the end of a REM episode gave the start for the following NREM episode. We have retained the first four NREM–REM cycles for study.

Data Analysis
Time-courses of our own averaged data for 1 Hz bins in the region of the 18 Hz point of discontinuity were plotted to confirm that there effectively exists a fundamental change in comportment in this region, as suggested by the data in Figure 1. We then looked in greater detail at this by examining individual-subject real-time data for each of the four NREM–REM cycles as we moved upward in 1Hz steps through the frequency range 14–30 Hz. For each cycle, three criteria were used to locate the discontinuity. These criteria are based on the character of the discontinuity as seen in Figure 1 and on cellular level results (Steriade *et al.*, 1990) indicating that brainstem-induced activation processes in thalamic and cortical systems should be U-shaped in NREM, with a subsequent high plateau in REM:

- the initial slope of the NREM time-course switches abruptly from positive (low start) to negative (high start);
- the final slope of the NREM time-course switches abruptly from negative to positive;
- the ratio of central trough minimum NREM power to average REM power changes abruptly from significantly greater to significantly less than unity.

For each criterion the result was decided by direct visual examination and assigned as true, false or indeterminate. The centre frequency between true and false was taken as the discontinuity frequency. Descriptive statistics were used to quantify the results. The histograms of counts for each of the three criteria used to determine the discontinuity frequency were checked separately for normality using Rankit plots. Using the discontinuity frequency variable, a repeated measures analysis of variance (ANOVA) with two trial factors (criteria and cycle number) was carried out to determine whether within subjects there was any statistical difference in the discontinuity frequency across the four cycles and over the three criteria. To protect against violation of the required compound symmetry assumption, the Greenhouse–Geiser adjustment of the probability was used and the result crosschecked by multivariate repeated measures analysis that does not require compound symmetry.
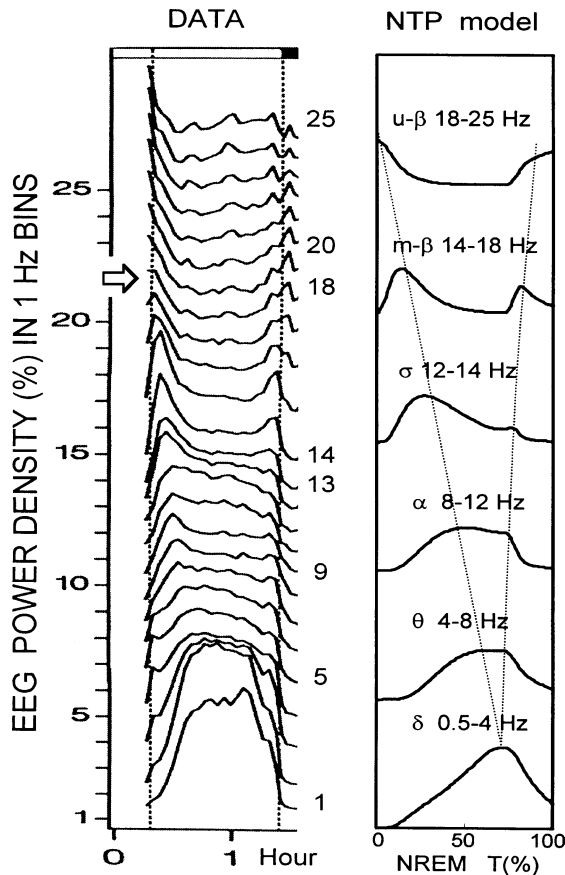
Figure 1. Left hand panel: average power time-course data in 1 Hz bins in NREM 1, showing the continuum of time-course shapes from 1 to 25 Hz (delta to high beta), broken only by the evident discontinuity in starting slope at ~18 Hz (indicated by an arrow). The start of REM sleep is indicated by a filled horizontal bar at the top. Adapted from Aeschbach and Borbély (1993), by kind permission of the publishers. The right hand panel shows that the NTP model can simulate this continuum: the positions of the maxima fall on smoothly continuous loci extending throughout the frequency range.

After verifying the general homogeneity of the data over the night and over the three criteria, all data for the 18 subjects were combined and a histogram of frequencies at which discontinuity occurs enabled the extraction of the general average and standard deviation for the location of the discontinuity. In order to highlight the difference in time-course shapes, the traditional beta band was then split into two ranges (U-shaped and M-shaped) at this point and the time-courses plotted for each range and for each NREM–REM cycle. This was done on averaged data using all 18 subjects. Since it is not possible to combine meaningfully real-time time-courses due to the large inter-subject variation in episode duration, we standardized each NREM and REM duration to 100% and calculated average power in each 2% (NREM) and 5% (REM) time bin. These were then recombined taking account of the real-time NREM and REM durations to give plots over the entire cycle. Additionally, the overnight trends of integrated power in the U and M ranges were compared using orthogonal-polynomial repeated measures ANOVA. This was done separately for the NREM and for the REM episodes.

Principle component analysis (PCA) and hierarchical cluster analysis were then applied as an additional check. PCA — used in the past to assign band limits (e.g. Corsi-Cabrera *et al.*, 2000; De Gennaro *et al.*, 2001, 2002) — was carried out across the four cycles on 1 Hz power values averaged over 18 subjects in the traditionally defined beta range to explore the homogeneity in this band. This statistical technique is used to reduce a large number of variables to a small set of derived variables (components or factors) with a minimum loss of information, so as to detect any underlying structure in the relationships between the

variables. This reduction is achieved by expressing inter-correlated variables as single factors. Hierarchical cluster analysis was carried out on the power values within 1 Hz bins extending over the sigma (10–15Hz) and the traditionally defined beta (15–25 Hz) ranges in order to explore any partiality in the bin assignment of the 15–18 Hz range to either sigma or beta. Average power for consecutive 1 Hz bins was computed over the four cycles and the distance (degree of dissimilarity) between all bin pairs assessed using the R^2 metric computed as 1 minus the squared Pearson product moment correlation coefficient between each pair of objects (1 Hz bins). The bins were then joined using the Ward minimum variance algorithm, giving rise to a hierarchical tree. Statistical analyses were carried out using SYSTAT software.

Results

An overview of all night sleep as measured by standard sleep stage variables indicates that the quality of sleep for the subjects studied is well within the normal range. Sleep latency, defined as the interval between lights out and the first occurrence of stage 2, was 15.2 ± 2.6 (SEM) min. The latency from stage 2 to REM sleep was 82.4 ± 7.0 min. Duration variables were also in the norm, with 32.0 ± 2.5, 252.7 ± 8.8, 101.3 ± 10.1 and 116.8 ± 4.8 min of stages 1, 2, slow wave sleep (stages 3 + 4) and REM sleep, respectively, giving a total sleep time duration of 502.8 ± 4.8 min. The duration of waking intervals within sleep (i.e. after sleep onset) was 10.3 ± 1.4 min giving a sleep efficiency index, defined as the ratio of total sleep time (excluding waking intervals) to total sleep period (including waking intervals), of 0.98 ± 0.003.

Figure 2 gives for the first NREM–REM cycle a clear confirmation of the discontinuity in time-course shape at ~18 Hz originally indicated by the data in Figure 1. The time-courses for the 1 Hz bins in the interval 14–20 Hz, for data averaged over 18 subjects, show an abrupt change within NREM from M-shaped below 18 Hz to U-shaped above 18 Hz, and an accompanying change in the REM plateau level from low to high. It is remarkable that this phenomenon is totally invisible in the power-frequency spectrum where no discontinuity occurs in the region of 18 Hz. The spectrum over the range 14–20 Hz can be obtained by integrating the power over the time-courses in Figure 2. We obtain the mean values 6.5, 3.8, 2.4, 1.9, 1.7 and 1.5 $\mu V^2/Hz$ respectively for the six 1 Hz bins. These show a smooth ~1/f decrease with no discontinuity, despite the sharp discontinuity in time-course shape at ~18 Hz.

Figure 3 shows examples of 1 Hz bin time-courses for two typical subjects to illustrate the data used to determine more precisely the point of time-course discontinuity and to show that this point varies considerably from one subject to another. In straightforward cases like these, which constitute 80% of the total measured over the four NREM–REM cycles, the U to M discontinuity is evident from one 1 Hz bin to the next — showing that discontinuity takes place in less than ~1 Hz. In these cases the discontinuity frequency is taken as the integer frequency separating the two bins. In 12% of the cases, M- and U-type bins are separated by one bin of indeterminate time-course shape and in 8% by two. For these the discontinuity frequencies are calculated as the centre of the indeterminate interval. In 36% of the cases the three criteria agree exactly on the assignment of the discontinuity frequency. In 50%, two of the three agree, and in all cases the three agree within 1 Hz. Although the discontinuity frequency varies considerably between subjects, repeated measures ANOVA results show that within subjects there is no significant variation either overnight over the four NREM–REM cycles [$F(3,51) = 1.48$, $P = 0.24$] or
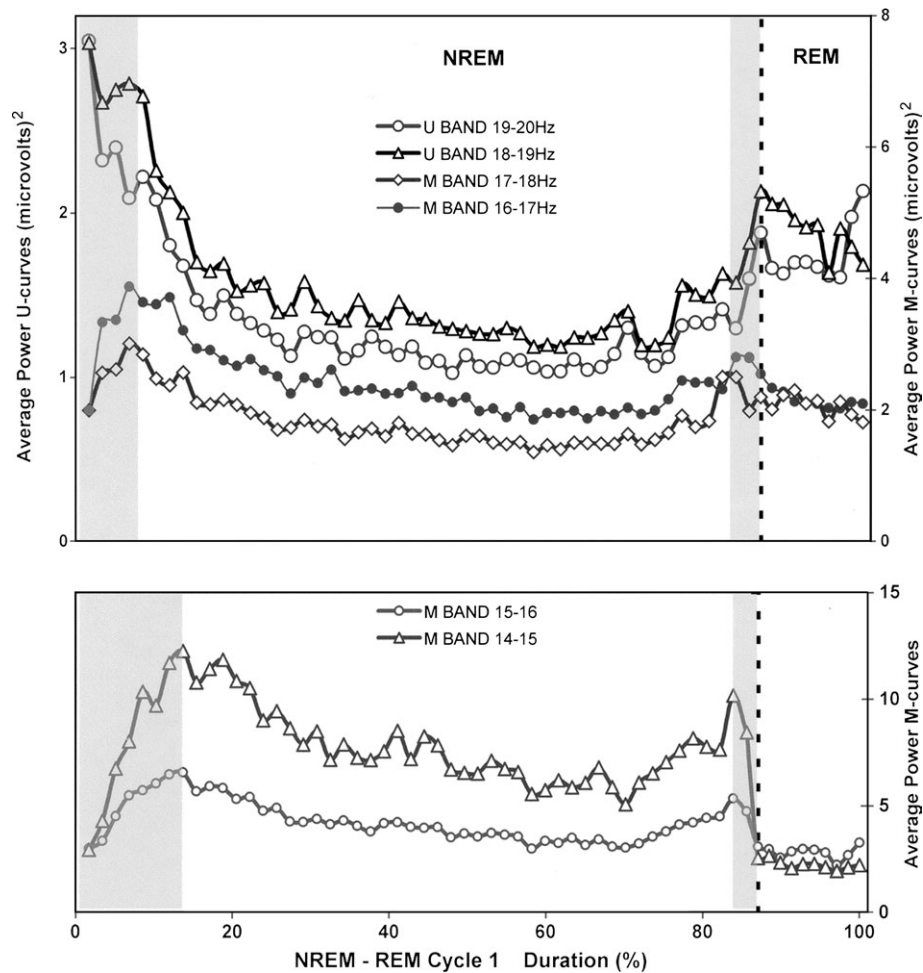
Figure 2. 1 Hz bin power time-courses 16–17, 17–18, 18–19 and 19–20 Hz (upper panel) and 14–15, 15–16 Hz (lower panel) averaged over all 18 subjects across NREM–REM cycle 1. They show the change from M to U shape in NREM and the change from low to high plateau level in REM that occurs between the 17–18 and the 18–19 Hz bins. The shaded area indicates zones of opposite slope. The vertical dotted line indicates the transition from NREM to REM. See online supplementary material for a colour version of this figure.

over the three different criteria [$F(2,34) = 1.85$, $P = 0.18$], so that the results can be combined to give an overall mean and standard deviation of 18.1 ± 1.5 Hz. The histogram of discontinuity frequencies for all 18 subjects is shown in Figure 4.

As a consequence of this finding, and in view of the common practice of working with averaged data, the traditional beta band was split at 18 Hz and the averaged time-courses for 15–18 and 18–25 Hz plotted separately for each NREM–REM cycle. Figure 5 shows that for each of the four cycles the two time-courses are totally different in shape, the higher frequency range being U-shaped and the lower frequency range being M-shaped. The M-shaped curve falls to a level in REM well below its central minimum in NREM, while U beta rises to a level in REM well above its central minimum in NREM. These differences called for a closer look at the overnight trends of integrated power for the two. Overnight trends across the four NREM episodes were significant for both [$F(3,102) = 17.82$, $P < 0.0005$], but not significantly different between the two [$F(3,102) = 1.46$, $P = 0.24$]. The within subjects results indicate highly significant linear [$F(1,34) = 32.35$, $P < 0.0005$] and quadratic [$F(1,34) = 13.76$, $P = 0.001$] trends, the former accounting for 41% and the latter 56% of the variability across consecutive NREM episodes. Similarly, across the four REM

episodes for both U and M ranges a significant overnight trend [$F(3,102) = 5.57$, $P = 0.02$] was shown, with a significant overnight linear decline that accounts for 94% of the variability. Again, these trends were not significantly different between the two curve types [$F(3,102) = 0.85$, $P = 0.38$]. These results as a whole are compatible with previous overnight trend analyses based on single Hz data (Aeschbach and Borbély, 1993).

The placing of the discontinuity at 18 Hz is substantiated by PCA carried out on the beta range, which showed that frequencies above 18 Hz load highly on (are highly correlated with) factor 1 ($r \approx 0.95$), while those below load highly on factor 2 ($r \approx 0.87$). These first two factors explain 95.4% of the total variance. Finally, the degree of similarity between the 1 Hz bin time-courses, over the sigma and beta range, is shown in the cluster tree (Fig. 6), where frequencies above and below 18 Hz respectively form distinct clusters that are separated by the largest (2.5) inter-cluster distance. The figure also indicates that the cluster formed by frequencies below 18 Hz is less homogeneous than that formed by frequencies above, with the 16–18 Hz bins joining together segregated from the remaining members of the cluster by the second largest distance (1.3). Thus, at a distance of 1, three distinct clusters separate out: 18–26, 16–18 and 10–16 Hz.
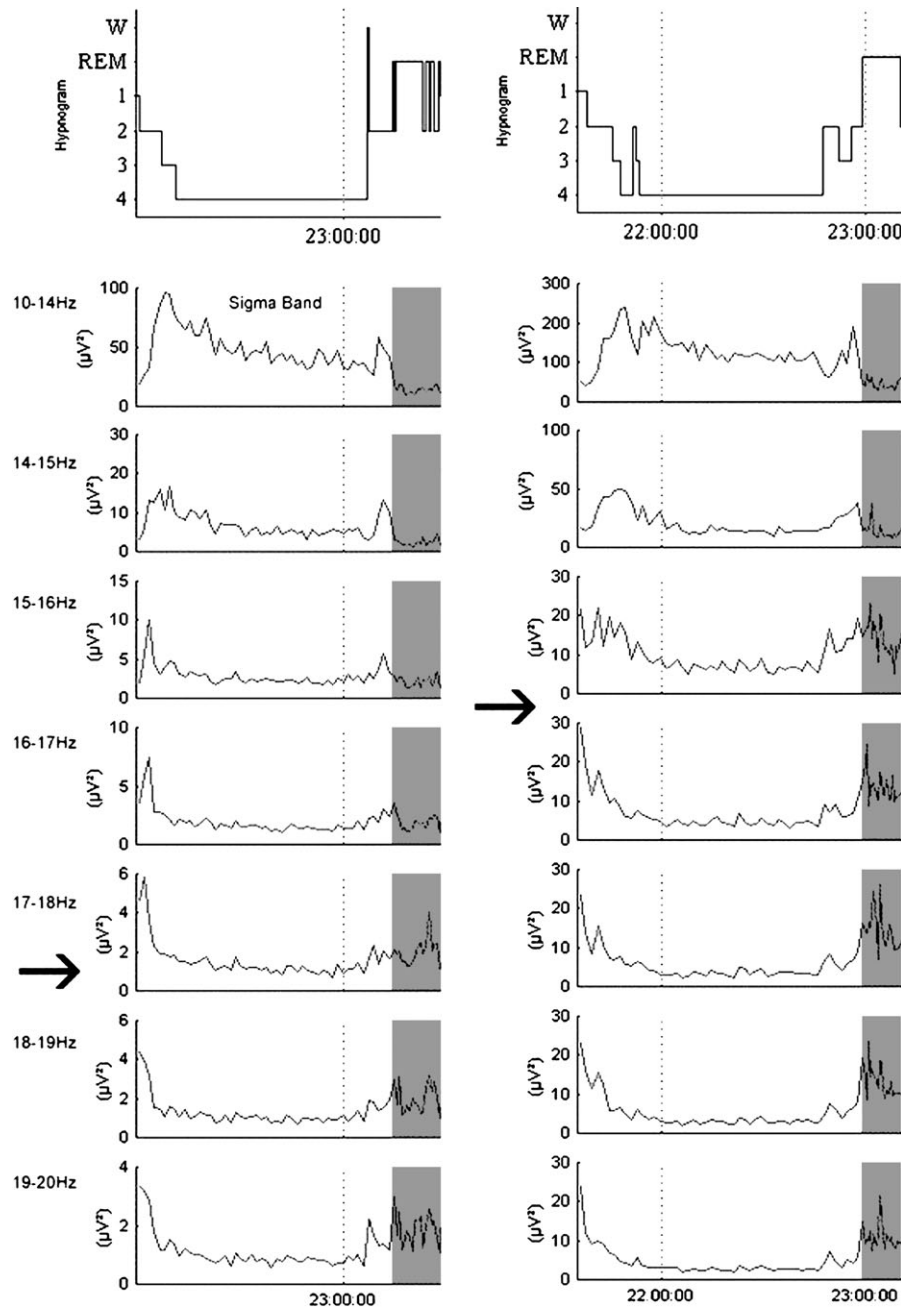
Figure 3. 1 Hz band power time-courses for two subjects across NREM–REM cycle 1, together with the corresponding hypnograms in the uppermost panels, as examples of the data used to determine the point of time-course discontinuity. They show how this point (indicated by an arrow) varies from one subject to another. W = wake; REM = REM sleep (grey-shaded); 1, 2, 3, 4 = NREM sleep stages. An initial stage 1 epoch represents the sleep onset period and sleep onset is defined as the first appearance of stage 2. For comparison the sigma band is also indicated.

Discussion

For the first time, a very sharp discontinuity in time-course shape as a function of frequency has been pointed out and measured in the beta range for the NREM–REM cycle. The practical implication of this finding is that the single beta band generally adopted until now has to be split at about 18 Hz to minimize distortion of the measured time-courses. This is in line with results reported by Uchida *et al.* (1992) on the reciprocal relation between beta and delta time-course shapes throughout the NREM–REM cycle, which showed consistency only above 20 Hz. This 20 Hz limit is well within two standard deviations of

our result ,and the 2 Hz difference may stem from the fact they use a 2 Hz resolution.

It is clear from Figure 5 that zones of opposite slopes at the start and end of the NREM episode render the two curve-types immiscible for the purpose of time-course analysis. Mixing the two in a single band, as done for the traditional beta band, can lead to ambiguous results which may render difficult, in particular, the study of sleep state transitions (sleep onset, REM onset, and REM offset). Since the lower frequencies of the beta band carry greater power than the higher (Fig. 2) they tend to contribute more to the overall shape of this band. It is this that

led to the incongruous results of De Gennaro *et al.* (2002), where beta power rises at the start of NREM and falls at the end — a result which is contrary to cellular neurophysiological findings reporting that the faster frequencies are enhanced during states of brain activation (REM sleep and wakefulness) and that this activation occurs minutes before entry into REM sleep (Steriade *et al.*, 1990, 1997).

The NTP model, fully described elsewhere (Merica and Fortune, 1997, 2000), places the observed discontinuity in a physiological context. Briefly, this model was conceived on the basis of findings on the generating mechanisms giving rise to

Figure 4. Histogram of the number of NREM start or end intervals of the time-courses for successive 1 Hz bands in which there is a slope reversal or in which the NREM trough to REM plateau ratio changes abruptly from greater than to less than unity. Data are from 18 subjects, each with four ultradian cycles and three criteria (216 intervals). See online supplementary material for a colour version of this figure.

the various sleep EEG rhythms, in particular the existence of different modes of oscillation of TC neurons under the modulatory control of brainstem–thalamic activating neurons (Steriade *et al.*, 1993a; McCormick and Bal, 1997). It postulates that the relationship observed between the time-courses of power in the different frequency bands of human sleep EEG, describing the progression of sleep states within the ultradian cycle is the result of stochastic transitions of the firing-rate frequencies of the brainstem–thalamic activating neurons: first a cascade of transitions towards and then a cascade away from deep sleep. The time-courses of the firing rates corresponding to each sleep state form a template that modulates both thalamic and cortical output. Consequently, at the thalamus the modulation results in identical cascades of frequency transitions of TC neurons: from beta to sigma to clock-like delta oscillatory mode in the sleep-deepening phase followed by the inverse cascade delta to sigma to beta in the sleep-lightening phase (Merica and Fortune, 2003). The cortically generated slow oscillation (<1 Hz) triggers shapes and synchronizes these thalamically generated cascades, forming at the cortex the complex wave sequences observed on the EEG (Steriade *et al.*, 1993b) from which the time-courses of power are extracted. The discontinuity of time-course shape with frequency is thus inherent in the model: the population of neurons of high firing-rate frequency present during brain activated states at NREM onset is the source of a cascade of frequency transitions to the lower frequencies present only in NREM. The depleting source implies a decreasing high-beta power and therefore a negative slope, while for any lower-frequency band power is increasing from zero and therefore has a positive slope. This discontinuity at the start of the NREM episode is accompanied by a similar but
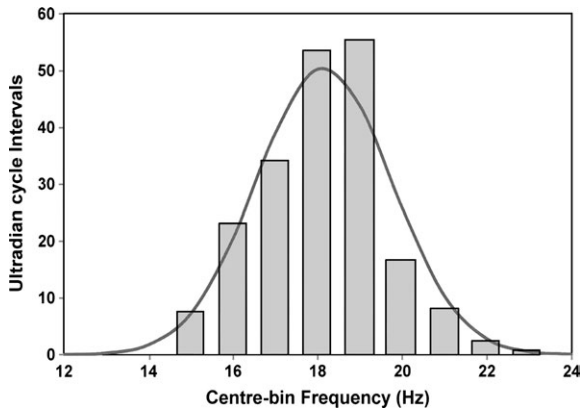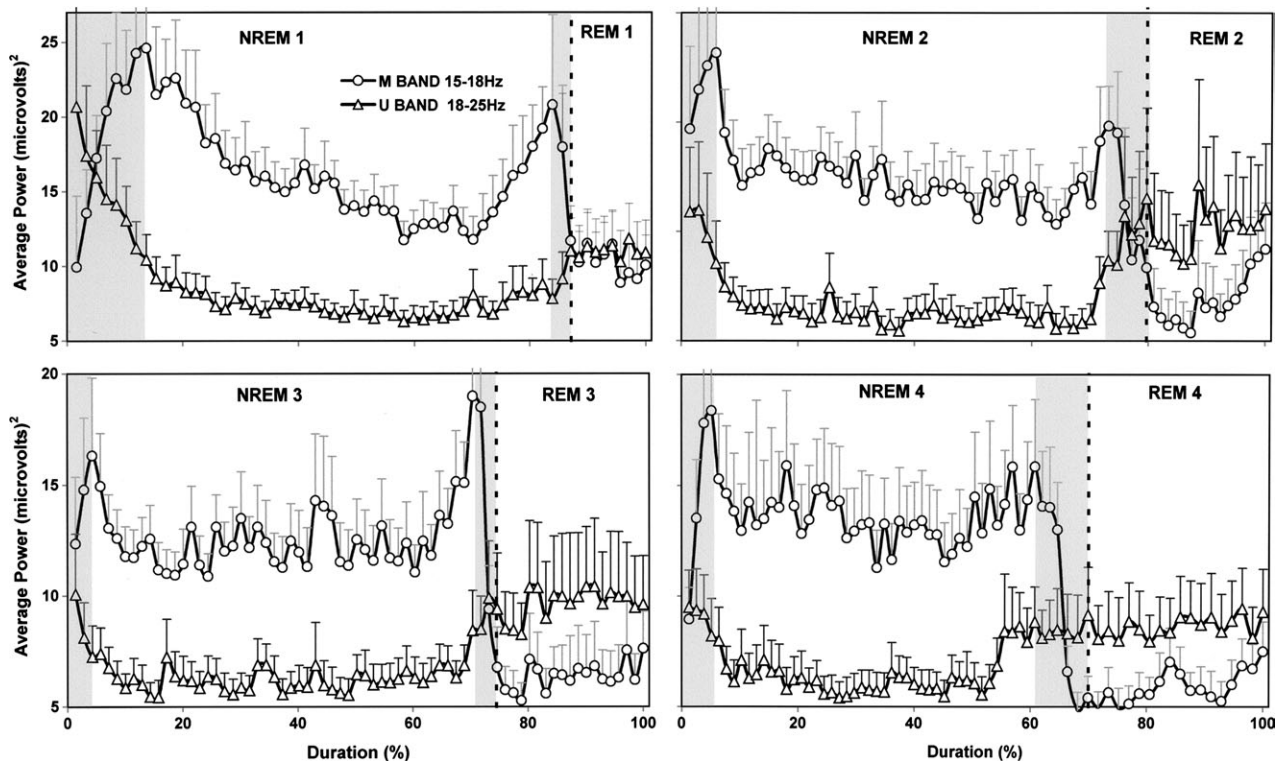

Figure 5. Power time courses of the M- (15–18 Hz) and U-shaped (18–25 Hz) bands averaged over 18 subjects for NREM–REM cycles 1–4. The shaded area indicates zones of opposite slope. The vertical dotted line indicates the transition from NREM to REM. A 10% resolution was adopted in the REM 1 episode to simplify the figure. See online supplementary material for a colour version of this figure.
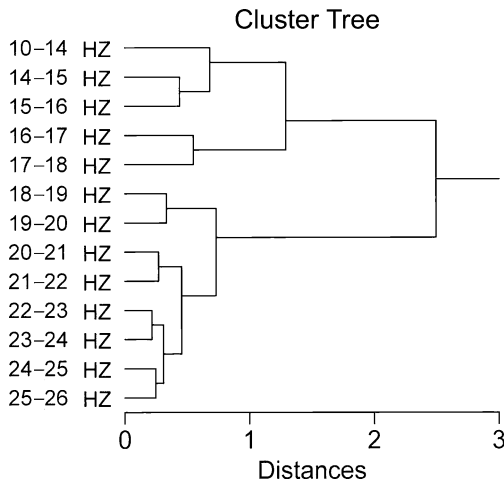
Cluster Tree

Figure 6. Cluster analysis of 1 Hz time-course bins over the beta and sigma ranges 14–26 Hz, together with the major portion of the sigma band (10–14 Hz) taken as a single bin. The distance scale below the tree shows the joining distance at each branch. At a distance of 1, three clusters separate out 18–26, 16–18 and 10–16 Hz.

inverse discontinuity at the end of it. The model reproduces with some precision the very particular relationship between power in the major frequency bands as seen in the human EEG, and also seen in cat data at both the thalamus and cortex (Lancel *et al.*, 1992). The neurophysiological findings on which the model is based are derived mainly from cat data, which comforts us in the belief that the model holds for all mammals from cats to humans. Similar time-course relations have not yet been confirmed for much smaller animals such as the rat (Bjorvatn *et al.*, 1998), where a detailed time-course analysis is difficult because of the polyphasic nature of rat sleep.

While our present results provoke a fundamental reassessment of the way in which the progression of power in the different frequency bands should be measured, they also raise the question of what the 15–18 Hz range represents. Is it an extension of the traditional sigma band (11–15 Hz), with which it has strong affinity in shape, or is it a low beta band specific to NREM sleep? To address this question, we turn again to evidence acquired at the cellular level, where it has been shown (Steriade *et al.* 1996; Steriade 2001) that fast frequency rhythms are voltage (depolarization)-dependent and therefore appear superimposed on the depolarizing phase of the cortically generated slow oscillation that is present only during NREM sleep. This grouping or coalescence of both the beta and spindle rhythms by the slow oscillation has also been confirmed in human sleep EEG (Mölle *et al.* 2002). Moreover, at the EEG we have direct measurement and therefore irrefutable evidence of the coexistence of all frequency bands at all times, albeit at different power levels, during the NREM episode (e.g. Fig. 1). These findings allow the view that the 15–18 Hz range may be a NREM-specific low beta band: it starts low at the onset of NREM and falls off before entry into REM.

There is, on the other hand, also support in favour of the sigma extension hypothesis. Two recent studies report the presence of fast spindles in healthy subjects: Anderer *et al.* (2001) in the frequency range 9.6–17.6 Hz and Nader *et al.* (2003) in the range 16–19 Hz. Further work is required to substantiate these findings since the majority of studies on spindle activity (Jobert *et al.*, 1992; Werth *et al.*, 1997; Zygierewicz *et al.*, 1999; Blinowska and Durka, 2001; Himanen

et al., 2002) suggest that spindles are relatively rare above 15 Hz. The shape of the 15–18 Hz range may also be a pointer to its identity. The two-peak shape of the sigma power time-course within NREM described by a number of authors (Lancel *et al.*, 1992; Aeschbach and Borbély, 1993, Dijk *et al.*, 1993 ; Uchida *et al.*, 1994; Merica and Blois, 1997) is similar to what we observe here in the 15–18 Hz range and very different from that of the upper (18–25Hz) beta range. The shape argument can be seen in the context of the continuum of shapes from delta through all bands up to high beta, broken only by the discontinuity at 18 Hz. Figure 1 shows this continuum and the NTP model simulation of it. The superposed loci of time-course maxima, despite the abrupt shape discontinuity at 18 Hz, are continuous all the way from the single-peak right-skewed delta to the fully separated double 'peak' of U-beta. The second sigma peak starts to separate out at ~13 Hz, so we could expect that if the sigma band did extend above 15 Hz it would have the more widely spaced and sharper peaks we actually see in the 15–18 Hz range. A final decision on whether this range represents spindles or beta oscillations or both must await measurement of the relative proportion of power manifested as high frequency spindles to that manifested as 'beta' oscillations not having spindle characteristics.

In conclusion, a hitherto unnoticed sharp discontinuity in sleep EEG time-course shape at 18.1 ± 1.5 Hz cannot be ignored if precise measurement is to be made of the progression of sleep states corresponding to different frequency bands on the sleep EEG. The importance of such precision is clear in the study of sleep-state transitions and when attempting to relate EEG time-courses to modulatory activity at subcortical level. Of perhaps greater importance, the discontinuity appears to be related to the fundamental physiology of sleep structure as described in the NTP model. The abrupt change of shape at ~18 Hz divides the higher neuronal oscillation frequencies 15–30 Hz into two categories: those that are specific to NREM sleep and those that are specific to the brain activated states wake and REM.

Supplementary Material

Supplementary material can be found at: http://www.cercor.oupjournals.org/.

Notes

Address correspondence to Helli Merica, Hôpitaux Universitaires de Genève, Belle Idée, Laboratoire de Sommeil et de Neurophysiologie, 2 Chemin du Petit Bel-Air, 1225 Chêne-Bourg, Geneva, Switzerland. Email: helli.merica@hcuge.ch.

References

Aeschbach D, Borbély AA (1993) All-night dynamics of human sleep EEG. J Sleep Res 2:70–81.

Amzica F, Steriade M (1998) Electrophysiological correlates of sleep delta waves. Electroencephal Clin Neurophysiol 107:69–83.

Anderer P, Klösch G, Gruber G, Trenker E, Pascual-Marqui RD, Zeitlhofer J, Barbanoj MJ, Rappelsberger P, Saletu B (2001) Low-resolution brain electromagnetic tomography revealed simultaneously active frontal and parietal sleep spindle sources in the human cortex. Neuroscience 103:581–592.

Bjorvatn B, Fagerland S, Ursin R (1998) EEG power densities (0.5–20 Hz) in different sleep-wake stages in rats. Physiol Behav 63:413–417.

Blinowska KJ, Durka PJ (2001) Unbiased high resolution method of EEG analysis in time-frequency space. Acta Neurobiol Exp 61:157–174.

Corsi-Cabrera M, Guevara MA, Del Rio-Portilla Y, Arce C, Villanueva-Hernandez Y (2000) EEG bands during wakefulness, slow-wave and paradoxical sleep as a result of principal component analysis in man. Sleep 23:738-744.

De Gennaro L, Ferrara M, Bertini M (2001) The boundary between wakefulness and sleep: quantitative electroencephalographic changes during the sleep onset period. Neuroscience 107:1-11.

De Gennaro L, Ferrara M, Curcio G, Cristiani R, Bertini M (2002) Cortical EEG topography of REM onset:the posterior dominance of middle and high frequencies. Clin Neurophysiol 113:561-570.

Dijk D, Hayes B, Czeisler CA (1993) Dynamics of electroencephol-graphic sleep spindles and slow wave activity in men: effect of sleep deprivation. Brain Res 626:190-199.

Feinberg I, Floyd TC (1979) Systematic trends across the night in human sleep cycles. Psychophysiology 16:283-291.

Finelli LA, Borbély AA, Achermann P (2001) Functional topography of the human nonREM sleep electroencephalogram. Eur J Neurosci 13:2282-2290.

Himanen S-L, Virkkala J, Huhtala H, Hasan J (2002) Spindle frequencies in sleep EEG show U-shape within first four NREM episodes. J Sleep Res 11:35-42.

Jobert M, Poiseau E, Jähnig P, Schulz H, Kubicki S (1992) Topographical analysis of sleep spindle activity. Neuropsychobiology 26:210-217.

Lancel M, van Riezen H, Glatt A (1992) The time-course of sigma activity and slow-wave activity during NREMS in cortical and thalamic EEG of the cat during baseline and after 12 hours of wakefulness. Brain Res 596:285-295.

Lanquart JP (1998) Contribution to the definition of the power bands limits of sleep EEG by linear prediction. Comput Biomed Res 31:100-111.

Mann K, Bäcker P, Röschke J (1993) Dynamical properties of the sleep EEG in different frequency bands. Int J Neurosci 73:161-169.

McCormick DA, Bal T (1997) Sleep and arousal: thalamocortical mechanisms. Annu Rev Neurosci 20:185-215.

Merica H, Gaillard JM (1991) A study of the interrupted REM episode. Physiol Behav 50:1153-1159.

Merica H, Blois R (1997) Relationship between the time courses of power in the frequency bands of human sleep EEG. Neurophysiol Clin 27:116-128.

Merica H, Fortune RD (1997) A neuronal transition probability model for the evolution of power in the sigma and delta frequency bands of the sleep EEG. Physiol Behav 62:585-589.

Merica H, Fortune RD (2000) Brainstem origin for a new very slow (1 mHz) oscillation in the human Non-REM sleep episode. Sleep Res Online 3:53-59.

Merica H, Fortune RD (2003) A unique pattern of sleep structure is found to be identical at all cortical sites: a neurobiological interpretation. Cerebr Cortex 13:1044-1050.

Merica H, Fortune RD (2004) State transitions between wake and sleep, and within the ultradian cycle, with focus on the link to neuronal activity. Invited review for Sleep Med Rev (in press).

Mölle M, Marshall L, Gais S, Born J (2002) Grouping of spindle activity during slow oscillations in human non-rapid eye movement sleep. J Neurosci 22:10941-10947.

Nader RS, Smith CT, Muir D, Scharfe E (2003) The existence of 'super-fast' spindles in adolescent girls. Sleep 26(suppl):A73.

Rechtschaffen A, Kales AA (1968) A manual of standardized terminology, techniques and scoring system for sleep stages of human subjects. Los Angeles, CA: UCLA Brain Information Service/Brain Research Institute.

Saper CB, Chou TC, Scammell TE (2001) The sleep switch: hypothalamic control of sleep and wakefulness. Trends Neurosci 24:726-731.

Steriade M (1984) The excitatory-inhibitory response sequence of thalamic and neocortical cells: state-related changes and regulatory systems. In: Dynamic aspects of neocortical function (Edelman GM, Gall WE, Cowan WM, eds), pp. 107-157. New York: John Wiley.

Steriade M (2001) Impact of network activities on neuronal properties in corticothalamic systems. J Neurophysiol 86:1-39.

Steriade M, McCarley RW (1990) Brainstem control of wakefulness and sleep. New York: Plenum Press.

Steriade M, Datta S, Paré D, Oakson G, Curro Dossi R (1990) Neuronal activities in brain-stem cholinergic nuclei related to tonic activation processes in thalamocortical systems. J Neurosci 10:2541-2559.

Steriade M, McCormick DA, Sejnowski TJ (1993a) Thalamocortical oscillations in the sleeping and aroused brain. Science 262:679-685.

Steriade M, Nunez A, Amzica F (1993b) Intracellular analysis of relations between the slow (<1 Hz) neocortical oscillation and other rhythms of the electroencephalogram. J Neurosci 13:3266-3283.

Steriade M, Amzica F, Contreras D (1996) Synchronization of fast (30–40 Hz) spontaneous cortical rhythms during brain activation. J Neurosci 16:392-417.

Steriade M, Jones EG, McCormick DA (1997) Diffuse regulatory systems of the thalamus. In: Thalamus. Vol. 1. Organisation and function, pp. 269-338. Oxford: Elsevier Science.

Szymusiak R, Alam N, Steininger T, McGinty D (1998) Sleep-waking discharge patterns of ventrolateral preoptic/anterior hypothalamic neurons in rats. Brain Res 803:178-188.

Uchida S, Maloney T, Feinberg I (1992) Beta (20-28 Hz) and delta (0.3-3 Hz) EEGs oscillate reciprocally across NREM and REM sleep. Sleep 15:352-358.

Uchida S, Atsumi Y, Kojima T (1994) Dynamic relationships between sleep spindles and delta waves during a NREM period. Brain Res Bull 33:351-355.

Werth E, Achermann P, Dijk D, Borbély AA (1997) Spindle frequency activity in the sleep EEG:individual differences and topographic distribution. Electroenceph Clin Neurophysiol 103:535-542.

Zygierewicz J, Blinowska KJ, Durka PJ, Szelenberger W, Niemcewicz S, Androsiuk W (1999) High resolution study of sleep spindles. Clin Neurophysiol 110:2136-2147.